

Fast Quantitative Single-Molecule Detection at Ultralow Concentrations

Philippe Haas,[†] Patrick Then,[‡] Andreas Wild,[†] Wilfried Grange,[§] Sylvain Zorman,[§] Martin Hegner,^{||} Michel Calame,[⊥] Ueli Aebi,[⊗] Josef Flammer,[○] and Bert Hecht^{*,‡}

National Center of Competence for Research in Nanoscale Science (NCCR), Institute of Physics, Klingelbergstrasse 82, CH-4056 Basel, Switzerland, Nano-Optics & Biophotonics Group, Physikalisches Institut, Wilhelm-Conrad-Röntgen-Center for Complex Material Systems (RCCM), Experimentelle Physik 5, Am Hubland, 97074 Würzburg, Germany, Institut Jacques Monod, 15 Rue Hélène Brion, 75013 Paris, France, Centre for Research on Adaptive Nanostructures and Nanodevices, College Green, Dublin 2, Ireland, Department of Physics, Klingelbergstrasse 82, CH-4056 Basel, Switzerland, Biozentrum, Klingelbergstrasse 50-70, CH-4056 Basel, Switzerland, and Universitätsaugenklinik, Mittlere Strasse 91, CH-4031 Basel, Switzerland

The applicability of single-molecule fluorescence assays in liquids is limited by diffusion to concentrations in the low picomolar range. Here, we demonstrate quantitative single-molecule detection at attomolar concentrations within 1 min by excitation and detection of fluorescence through a single-mode optical fiber in presence of turbulent flow. The combination of high detectability and short measurement times promises applications in ultrasensitive assays, sensors, and point-of-care medical diagnostics.

The possibility to detect single fluorescent dye molecules and quantum dots in solution using fluorescence techniques is widely exploited in fluorescence correlation spectroscopy¹ as well as in assay applications.^{2–4} To achieve single-molecule detection, it is important to minimize background signals by using a small active volume and to optimize the overall photon detection efficiency. For single-molecule assays in solution, considering free diffusion only, the time between two successive single-molecule detection events increases inversely proportional to the concentration. We estimate that the average time it takes between two individual molecules in a 1 fM solution to reach a ~10 fL-detection volume, assuming 3D Brownian motion, is already on the order of several tens of minutes (part 1 of the Supporting Information). This poses a practical lower limit of workable concentrations for real-time single-molecule detection assays based on diffusion in solutions in the low picomolar range and necessitates long incubation times for surface bound assays.⁵ One way to overcome this diffusion

limit is to vigorously stir the sample such that conditions for turbulent flow are created. Here, we demonstrate that it is possible to detect single molecules in solutions with nominal concentrations down to the attomolar range by excitation and detection of single-molecule fluorescence through a cleaved single-mode optical fiber in the presence of turbulence. Because of the resulting fast transport and rapid mixing within the sample solution, typical measurement times in this study are as low as 1 min. While the detection of fluorescence through the optical fibers of marked ligands immobilized to the fiber end has been demonstrated previously,^{6–8} detection of single molecules has not been achieved so far although it was proposed earlier.⁹ Our approach combines for the first time the power of single-molecule detection with the ability to quantitatively detect ultralow analyte concentrations in short times. In combination with suitable fluorescent probes, this opens up a plethora of possible applications in molecular biology and medical diagnostics. In particular, the small dimensions and flexibility of optical fibers and the short measurement time suggest applications in restricted geometries, point-of-care diagnostics, and in time-critical assays. Specifically this may include direct, on-site, and real-time detection of viruses by means of their specific DNA, the detection of other pathogens including proteins, real-time monitoring of rare but important marker molecules in medical applications, or mobile environmental ultrasensing.

The experimental setup is depicted schematically in Figure 1A (for further details see Methods in the Supporting Information). To minimize the background, we optimize the system for fluorescence detection in the near-infrared (750–830 nm), as few naturally occurring compounds emit fluorescence above 600 nm.² The excitation light (635 nm, 2mW at the fiber exit) is transmitted through a 20–30 cm length of optical fiber and emitted via a 90°-cleaved fiber end into the liquid sample volume. Here it excites single molecules to saturation whose fluorescence is coupled back into the fiber if they reside in the detection volume. The fiber end's collection efficiency is estimated to be about 10× smaller

* To whom correspondence should be addressed. E-mail: hecht@physik.uni-wuerzburg.de.

[†] NCCR, University of Basel.

[‡] Universität Würzburg.

[§] Université Paris 7 et CNRS.

^{||} Trinity College.

[⊥] Department of Physics, University of Basel.

[⊗] Biozentrum, University of Basel.

[○] Universitätsaugenklinik, University of Basel.

- (1) Kim, S. A.; Heinze, K. G.; Schwille, P. *Nat. Methods* **2007**, *4*, 963–973.
- (2) Zander, C.; Enderlein, J.; Keller, R. *Single Molecule Detection in Solution: Methods and Applications*; Wiley-VCH: Berlin, Germany, 2002.
- (3) Sauer, M.; Drexhage, K.; Zander, C.; Wolfrum, J. *Chem. Phys. Lett.* **1996**, *254*, 223–228.
- (4) Wolfbeis, O. *Anal. Chem.* **2000**, *72*, 81R–89R.
- (5) Schena, M.; Shalon, D.; Davis, R.; Brown, P. *Science* **1995**, *270*, 467.

(6) Tan, X.; Liu, W. *Anal. Chem.* **1999**, *71*, 5054–5059.

(7) Walt, F.; Steemers, J.; Ferguson, J. *Nat. Biotechnol.* **2000**, *18*, 91–94.

(8) Ferguson, J.; Boles, T. *Nat. Biotechnol.* **1996**, *14*, 1681–1684.

(9) Hecht, B.; Haas, P.; Wild, A.; Hegner, M.; Calame, M. Single analyte molecule detection by fibre fluorescence probe. U.S. Patent 7,657,133, February 2, 2010.

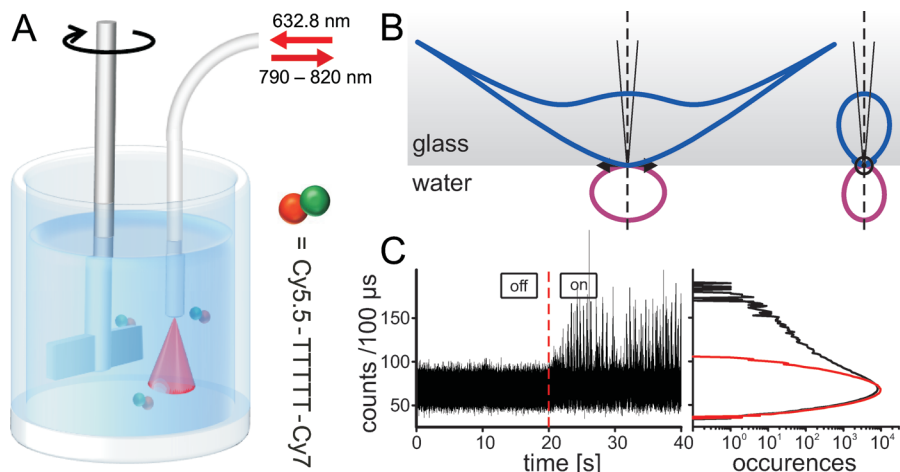


Figure 1. Principle of quantitative single-molecule detection at ultralow concentrations using excitation at 635 nm and fluorescence detection at 790–820 nm: (A) schematic experimental setup showing the analyte container with the optical fiber positioned close to the rotor blades and some analyte molecules (green-red dots, see the text and Methods in the Supporting Information). (B) Blue line: cuts through the distorted emission pattern of a single dipole emitter oriented parallel and close to the water/glass boundary at the cleaved fiber end (gray box) along the dipole and perpendicular to the dipole indicated by the black arrows. Only photons emitted into a small angular range (as indicated by the two thin lines next to the dashed surface normal) are transmitted to the detector. (C) Fluorescence time trace recorded from a 10 pM solution showing the difference between rotor off (0–20 s) and on (20–40 s), respectively. Left panel: corresponding histograms calculated separately for rotor on (black trace) and off (red trace) showing a deviation from the Poisson distribution only for the rotor on case.

than that of a 0.5 NA microscope objective. We take into account that in proximity of a plane interface, like the water–glass boundary at the fiber end, the emission pattern of dye molecules changes from the well-known dipolar pattern of a free dipole to an emission pattern which directs the majority of photons into the optical denser medium.¹⁰ Representative emission patterns for the main dipole orientations are displayed in Figure 1B. However, only photons radiated within the angular range suitable for total internal reflection in the fiber are transmitted to the detector. For the present geometry and assuming the molecule to be close to the fiber end, this accounts for about 0.3% of the total emission by the molecule¹¹ (part 2 of the Supporting Information).

The use of a single-mode fiber as an optical transducer is hindered by background generated due to inelastic scattering processes in the fiber exhibiting a spectrum extending ~ 100 nm beyond the excitation wavelength. The fiber background is proportional to the intensity coupled into the fiber as well as to the length of the fiber. For fiber lengths of 30 cm, this generic background could already prevent successful single-molecule detection using standard dye molecules with their typically rather small Stokes shift. However, the Stokes shift can be increased by using a covalently linked donor–acceptor pair of dye molecules exhibiting efficient fluorescence resonant energy transfer (FRET) or suitably chosen colloidal semiconductor quantum dots. Here we use a Förster pair consisting of five thymidine bases connecting a Cy5.5 molecule at the 3' end and a Cy7 molecule at the 5' end (Cy5.5-TTTTT-Cy7, Genelink and Microsynth). The Förster pair is excited at a wavelength of 635 nm while the emission maximum for Cy7 occurs at 767 nm, well within the setup's detection bandwidth (see part 3 of the Supporting Information).

Figure 1C displays a time trace of fluorescence with a binning time of 100 μ s recorded from a 10 pM dye solution with the rotor

initially turned off. The trace shows a constant level of background counts with a Poissonian distribution due to background generated in the fiber but no fluorescence bursts due to diffusing molecules. As soon as the stirring is switched on (after 20 s), fluorescence bursts appear at a high rate and the histogram deviates from a Poissonian distribution. It may be noted that the signal-to-noise ratio seems to be unusually small compared to conventional single-molecule experiments. However, because of the fact that the fluorescence bursts can be clearly distinguished from the Poissonian background, detection of single-molecule events is possible with high efficiency (see ref 12). Small improvements of the signal-to-noise ratio will lead to a further increased detectability. Since molecules can only be efficiently collected if they reside within a small volume close to the fiber end (10 fL, see part 2 of the Supporting Information), diffusion is no longer sufficient at low concentrations (picomolar and below) to have a sufficient number of molecules passing the detection volume per unit time. In addition, excitation of molecules takes place in a much larger illuminated volume due to the Gaussian light beam emerging from the fiber end. Therefore, even for moderate concentrations, stirring is needed to ensure that enough molecules reach the detection volume before being bleached (Figure 1C, rotor off). We find that stirring at a rate of 20 000 rpm yields the best results if at the same time the relative position between the fiber and rotor is optimized (see part 4 of the Supporting Information). For the characteristic dimensions of the rotor (some 10^{-3} m) and the rather large velocities imposed by the stirring, Reynolds numbers of several thousands are easily achieved. The result is a highly turbulent flow in the sample volume which ensures rapid mixing.¹³ We suggest that the fiber end acts as a discontinuity in the flow profile, which leads to the formation

(12) Grange, W.; Haas, P.; Wild, A.; Calame, M.; Hegner, M.; Hecht, B. *J. Phys. Chem. B* **2008**, *112*, 7140–7144.

(13) Munson, B. R.; Young, D. F.; Okiishi, T. H. *Fundamentals of Fluid Mechanics*; John Wiley & Sons, Inc: New York, 2006.

(14) Soper, S. A.; Mattingly, Q. L.; Vegunta, P. *Anal. Chem.* **1993**, *65*, 740–747.

(10) Lukosz, W.; Kunz, R. *J. Opt. Soc. Am.* **1977**, *67*, 1615–1619.

(11) Novotny, L.; Hecht, B. *Principles of Nano-Optics*; Cambridge University Press: Cambridge, U.K., 2006.

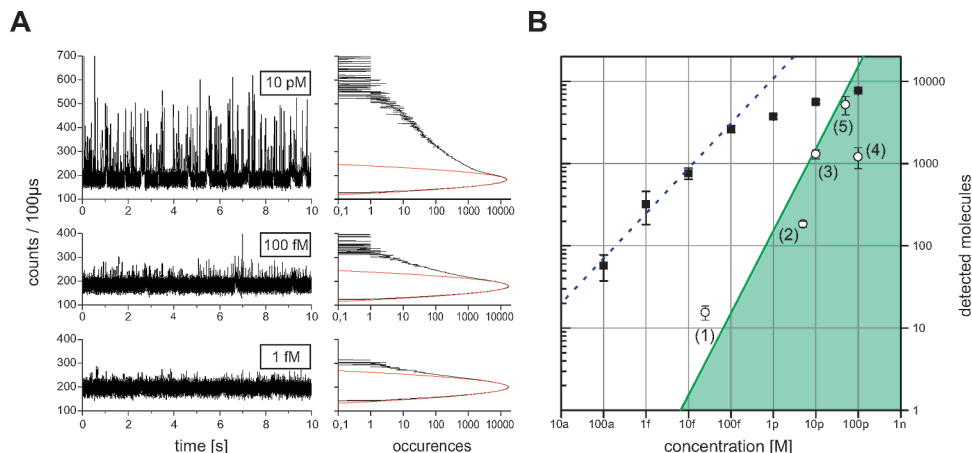


Figure 2. Dilution series: (A) Representative 10 s portions of 60 s time traces for different concentrations of dye molecules as indicated as well as respective histograms (black) with best fits to the Poissonian background (red) as needed for burst detection (part 1 of the Supporting Information). (B) ■, counted bursts above threshold as a function of the concentration measured within a 60 s integration time. A linear dependence is obtained between a concentration of 100 fM down to 100 aM (blue dashed line as guide-to-the-eye). Above 100 fM, the number of counted bursts deviates from linearity since bursts start to overlap in time (see ref 12 and part 5 in the Supporting Information). ○, Experimental data for diffusion-based assays taken from the literature (1,¹⁴ 2,¹⁵ 3,¹⁶ 4,³ and 5¹⁷). Note that ref 14 relies on active transport of analyte molecules through a capillary. All values have been scaled to a detection value of 10 fL. Solid green line and shaded area, theoretical upper limit and accessible area of the number of molecules entering the detection volume during 60 s considering Brownian motion only, see part 1 of the Supporting Information.

of additional vortices at the fiber end, which ensure the rapid exchange of fluorescent molecules in the detection volume at the fiber facet close to the core. The fact that detection of molecules for too low stirring rates is impossible indicates a sudden onset of vortex formation at the fiber end at rotor speeds of ~ 5000 rpm. The onset of vortex formation is also supported by an autocorrelation analysis of recorded time traces, which shows a broadening of the fluorescence bursts instead of a narrowing for higher stirring rates (see part 4 Figure 5b in the Supporting Information). These additional vortices do not appear in the vicinity of an infinitely extended boundary between liquid and glass which is encountered in detection schemes based on microscope objectives. In addition, the typical 200–300 μm working distances of high-numerical-aperture microscope objectives would limit the accessible detection range to low-velocity surface-bound flow sheets.

In order to demonstrate the possibility to detect ultrasmall concentrations of dye molecules within short measurement times of 60 s, a series of measurements have been performed for solutions with analyte concentrations varying over 6 orders of magnitude between 100 pM and 100 aM. Each acquired 60 s time trace is subjected to an analysis by a burst counting algorithm to determine the number of fluorescence bursts (see ref 12 and part 5 of the Supporting Information). Figure 2A shows typical 10 s portions of fluorescence time traces obtained from solutions containing analyte molecules in concentrations as indicated together with the respective histograms. For the higher concentrations (≥ 1 pM) the mean number of molecules that enter the detection volume per bin time is larger than one, causing occasional large count rates. In the corresponding histograms this leads to a pronounced deviation from the Poisson distributed background with a rather broad range of large amplitude bursts. With decreasing concentration, the number of detected fluorescence bursts decreases and the peak count rate above background observed in the histograms tends toward ~ 50 counts/100 μs limited by the saturation emission

rate of single Cy7 molecules and the maximum overall detection efficiency. At a concentration of 100 aM, the number of detected fluorescence burst is still on the order of several tens. This number does not only allow a reliable detection of single molecules at this concentration but lets one reasonably envision an extension of the technique to even lower concentrations. Quite remarkably, 100 aM is already about 1000 \times smaller than the smallest concentration reported in the literature for diffusion-based single-molecule detection.^{3,15–17} Figure 2B summarizes the results obtained by measuring a dilution series with our fiber-based setup. As a reference we also plot values for conventional diffusion-based single-molecule detection experiments in solution as reported in the literature. Furthermore, we plot the expected number of molecules that enter the detection volume within 60 s due to Brownian motion only as a function of the concentration (solid green line) according to the discussion in part 1 of the Supporting Information. This line describes the upper limit for the number of detected molecules during 60 s in a conventional diffusion-based single-molecule assay while the shaded area designates the regime accessible to conventional single-molecule detection assays. In conclusion, we clearly demonstrate that by combining turbulent flow and detection through a finite-sized optical fiber the fundamental detectability limit of diffusion-based single-molecule detection assays can be overcome. As a result, we are able to report fast quantitative single-molecule detection down to concentrations of 100 aM.

ACKNOWLEDGMENT

The authors thank H.-J. Güntherodt, J.-S. Huang, A. Lieb, P. Reimann, M. Steinacher, and J. Oberg for valuable discus-

- (15) Schaffer, J.; Volkmer, A.; Eggeling, C.; Subramaniam, V.; Striker, G.; Seidel, C. *J. Phys. Chem. A* **1999**, *103*, 331–336.
 (16) Zander, C.; Sauer, M.; Drexhage, K.; Ko, D.; Schulz, A.; Wolfrum, J.; Brand, L.; Eggeling, C.; Seidel, C. *Appl. Phys. B: Laser Opt.* **1996**, *63*, 517–523.
 (17) Nie, S.; Chiu, D. T.; Zare, R. N. *Anal. Chem.* **1995**, *67*, 2849–2857.

sions and support. Financial support by the Swiss National Science Foundation via the National Center of Competence in Research (NCCR) in Nanoscale Science and a research professorship for one of the authors (B.H.) as well as by the LHW-Stiftung and the Wolfermann-Nägeli-Stiftung is gratefully acknowledged. P.H., P.T., and A.W. contributed equally to this work. P.H. and A.W. conceived the project, designed and performed experiments, and analyzed data. P.T. optimized the setup, performed experiments, analyzed data, and wrote the paper. W.G. and S.Z. provided the estimation for the Brownian motion limit of single-molecule detection. M.C. and M.H. provided experimental guidance. U.A. and J.F. coordinated the project. B.H. conceived and coordinated the project, designed experiments, and wrote the paper.

NOTE ADDED AFTER ASAP PUBLICATION

This paper was published on June 22, 2010 with an incomplete title. The revised version was published on July 14, 2010.

SUPPORTING INFORMATION AVAILABLE

Additional information as noted in text. This material is available free of charge via the Internet at <http://pubs.acs.org>.

Received for review March 26, 2010. Accepted June 7, 2010.

AC100779C

Supporting information for: Fast quantitative single-molecule detection at ultralow concentrations

- Supporting Information -

Philippe Haas,^{†,@} Patrick Then,^{‡,@} Andreas Wild,^{†,@} Wilfried Grange,[¶] Sylvain Zorman,[¶] Martin Hegner,[§] Michel Calame,^{||} Ueli Aebi,[⊥] Josef Flammer,[#] and Bert Hecht^{*,‡}

*National Center of Competence for Research in Nanoscale Science (NCCR), Institute of Physics,
Klingelbergstr. 82, CH-4056 Basel, Switzerland, Nano-Optics & Biophotonics Group,
Physikalisches Institut, Wilhelm-Conrad-Röntgen-Center for Complex Material Systems (RCCM),
Experimentelle Physik 5, Am Hubland, 97074 Würzburg, Germany, Institut Jacques Monod, 15
rue Hélène Brion, 75013 Paris, France, Centre for Research on Adaptive Nanostructures and
Nanodevices, College Green, Dublin 2, Ireland, Klingelbergstrasse 82, CH-4056 Basel,
Switzerland, Klingelbergstrasse 50-70, CH-4056 Basel, Switzerland, and Mittlere Strasse 91,
CH-4031 Basel, Switzerland*

E-mail: hecht@physik.uni-wuerzburg.de

*To whom correspondence should be addressed

[†]NCCR, University of Basel

[‡]Universität Würzburg

[¶]Université Paris 7 et CNRS

[§]Trinity College Dublin

^{||}Department of Physics, University of Basel

[⊥]Biozentrum, University of Basel

[#]Universitätsaugenklinik, University of Basel

[@] authors contributed equally, alphabetical order

Supporting Information 1

Approximation of first passage time

For a concentration-independent diffusion coefficient D , Fick's (second) law states

$$\frac{\partial c}{\partial t} = D\nabla^2 c \quad (1)$$

Assuming the detection volume to be a sphere of radius a and rewriting 1 using spherical coordinates yields

$$\frac{\partial c}{\partial t} = D \frac{1}{r^2} \frac{\partial}{\partial r} \left(r^2 \frac{\partial c}{\partial r} \right). \quad (2)$$

For the stationary case this equation reads as

$$\frac{\partial c}{\partial t} = 0. \quad (3)$$

We now assume that the concentration within the detection volume is zero at any given time (i.e. once a molecule enters the detection volume, it is instantly bleached) and that the concentration is c_0 for $r \gg a$. The concentration can then be written as

$$c(r) = c_0 \left(1 - \frac{a}{r} \right). \quad (4)$$

Fick's first law can be used to calculate the diffusive flux J driven by a concentration gradient

$$J(a) = -D \frac{\partial c}{\partial r} \quad (5)$$

Calculating the total flux we get

$$J = 4\pi a D c_0 \quad (6)$$

which can be used to estimate the total number of molecules reaching the sphere during the time t by $J \times t$. The probability $P(k, \lambda)$ that there are k occurrences for an expected number of λ

occurrences during the time interval t is given by the Poisson distribution

$$P(k, Jt) = \frac{e^{-Jt} (Jt)^k}{k!} . \quad (7)$$

The average time it takes to observe a molecule corresponds to the average time for which no molecule is in the detection volume. The probability for zero molecules in a time interval t is

$$P(0, Jt) = e^{-Jt} . \quad (8)$$

The average time therefore reads as

$$\langle t \rangle = \frac{1}{\int_0^\infty P(0, Jt) dt} \cdot \int_0^\infty t P(0, Jt) dt = \frac{1}{4\pi a D c_0} . \quad (9)$$

In Figure 1 9 is used to calculate the average time it takes until a molecule reaches a 10 fl volume for different values of the diffusion coefficient D . For bigger molecules reasonable values for D range between $1 \cdot 10^{-10} \text{ m}^2/\text{s}$ and $5 \cdot 10^{-10} \text{ m}^2/\text{s}$. For this case, single molecule detection by diffusion will be limited to concentrations above roughly 10 fmol/l, as for lower concentrations the average time until a molecule will be detected quickly reaches several tens of minutes to hours.

Methods

The complete experimental setup is depicted in Figure 2. A semiconductor-diode-laser (**L**, IDT0-635-30, GMP, 30 mW) emitting at 635 nm is providing the excitation light. After passing through a filter wheel to control the power, the laser beam is deflected by a dichroic mirror (**1**, T740/140 650 dcip, Chroma) and coupled into a short (20 to 30 cm) piece of single-mode optical fiber (**F**, FS-SN-3224, $\lambda_{\text{cutoff}}=630 \text{ nm}$ and FS-SN-4224, $\lambda_{\text{cutoff}}=820 \text{ nm}$; Thorlabs). Fibers have been chosen for low Raman background. The light is transmitted through the fiber and emitted via a 90°-cleaved fiber end into the liquid sample volume **P**, where it excites single molecules whose

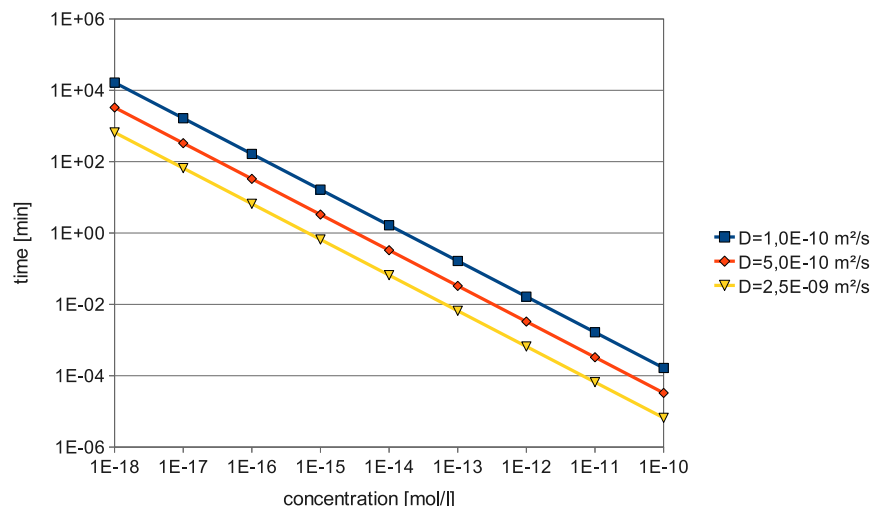


Figure 1: Average time until a molecule enters a 10 fl detection volume using equation 9. The diffusion coefficient has been chosen as $D = 1 \cdot 10^{-10} \text{ m}^2/\text{s}$ (squares), $D = 5 \cdot 10^{-10} \text{ m}^2/\text{s}$ (diamonds) and $D = 2,5 \cdot 10^{-9} \text{ m}^2/\text{s}$ (triangles), respectively.

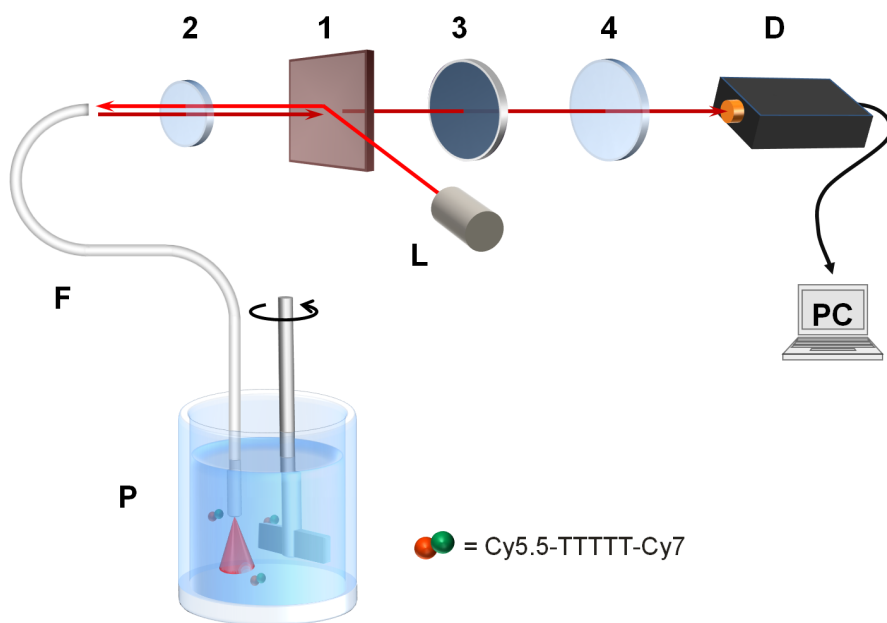


Figure 2: Schematic diagram of the experimental setup. L: Diode laser, 1: Dichroic mirror, 2: Microscope objective for fiber coupling, F: Short piece of single-mode optical fiber (20-30 cm), P: Sample container ($\phi=10 \text{ mm}$, $V=1 \text{ ml}$), 3: Bandpass filter, 4: Focusing lens, D: single-photon counting avalanche photodiode module.

fluorescence is coupled back into the fiber with sufficiently high efficiency. The fiber is connected to a computer controlled *xyz* positioner (I3005, Luminos Industries) which allows for a precise positioning of the fiber relative to the rotor. Best results were obtained when the fiber was slightly tilted into or out of the flow direction by $\sim 5\text{-}10^\circ$. All experiments were carried out using small concentrations of dye molecules dissolved in a buffer solution (10 mM TRIS-HCl, 50 mM KCl and 1.5 mM MgCl₂ in water, pH of 8.3). Wavelength-shifted single-molecule fluorescence after exiting the fiber passes the dichroic mirror, while residual excitation light traveling backwards through the fiber or being reflected at the fiber end facet gets deflected. The remaining light passes a bandpass filter (**3**, XF3307, Omega Optical) and is focused by a convex lens (**4**, $f=30$ cm) onto the active area ($\phi=180$ μm) of a single photon counting avalanche diode (**D**, SPCM-AQR-13, Perkin Elmer, quantum efficiency at 780 nm $\approx 60\%$) whose output is fed into a PC and evaluated by counting fluorescence bursts in the fluorescence time traces using a custom-made software (Labview, National Instruments) as described in **Supporting Information 5**. The focal length has been chosen such that the image of the fiber core fits the active area of the detector thus preventing excess background originating from cladding modes from reaching the detector's active area.

Supporting Information 2

Detection efficiency

The detection efficiency of the setup is dominated by the collection efficiency of the optical fiber. To calculate the percentage of light emitted by a dye molecule that is coupled into the fiber, we model an electric dipole close to a plane interface between two dielectric media (water: $n_1 = 1.33$ and glass: $n_2 = 1.54$). As the parallel orientation to the plane interface has a much higher statistical weight as opposed to the perpendicular orientation, we limit our analysis to parallel oriented dipoles. For a detailed analysis, the interested reader is referred to¹ and². Here we only present the results of the calculation.

If a dipole is located close to a plane interface between two dielectric media of different index

of refraction, the majority of the dipole emission will be coupled into the higher refractive index material. However, for an optical fiber, only the fraction of light entering the fiber up to the critical angle for total internal reflection within the fiber will couple to the fibers' guided mode. This angle can be calculated using the numerical aperture $NA = n \cdot \sin(\theta_1)$ of the optical fiber. By using Snell's law we find the maximum angle for light to be transported through the fiber by total internal reflection:

$$\sin(\theta_2) = \frac{1}{n_2} \cdot NA . \quad (10)$$

Therefore, for $NA=0.12$, only light that is propagating in the fiber with a maximum angle of $\pm 4.47^\circ$ can be transported through the fiber. This yields a fraction of 0.3% of the light emitted by a molecule. It should be noted that this value is independent of the distance of the dipole to the plane interface, as the distance affects only the amount of evanescent waves coupled into the second medium. However, as the equation used to calculate the emission pattern assumes an infinite plane, it is to be expected that the results are valid only for molecules sufficiently close to the interface. Furthermore, the molecules have to be close to the core of the fiber. Both factors limit the detection volume to approximately 10 femtoliters. Neglecting comparably minor losses in the lenses and the dichroic mirror, additional losses mostly occur at the bandpass-filter (transmission $\sim 80\%$) and at the detector (quantum yield at 780 nm $\sim 60\%$). Consequently, the total detection efficiency is estimated to $\sim 0.15\%$.

Supporting Information 3

FRET dyes

The dyes used in this work were Cy5.5 and Cy7, a well-known FRET, pair linked by 5 thymidine bases (Cy5.5-TTTTT-Cy7). The thymidine bases have been chosen because they exhibit low quenching of the fluorescence emission^{3,4}. Figure 3 shows normalized spectra of the light leaving the fiber together with the transmission curve of the bandpass filter. The bandpass filter is matched to the emission band of Cy7. The spectrum of the background was recorded with the fiber

end in air, while the spectra of Cy5.5 and Cy7 were recorded when dipping the fiber in solutions containing sufficiently large concentrations of the pure dyes. Using a bandpass filter with high transmission around 800 nm largely suppresses the background generated in the fiber while transmitting most of the acceptor fluorescence. A main advantage of the Cy5.5-Cy7 pair is the acceptor emission in the NIR spectral range, as few naturally occurring compounds emit light in this range.

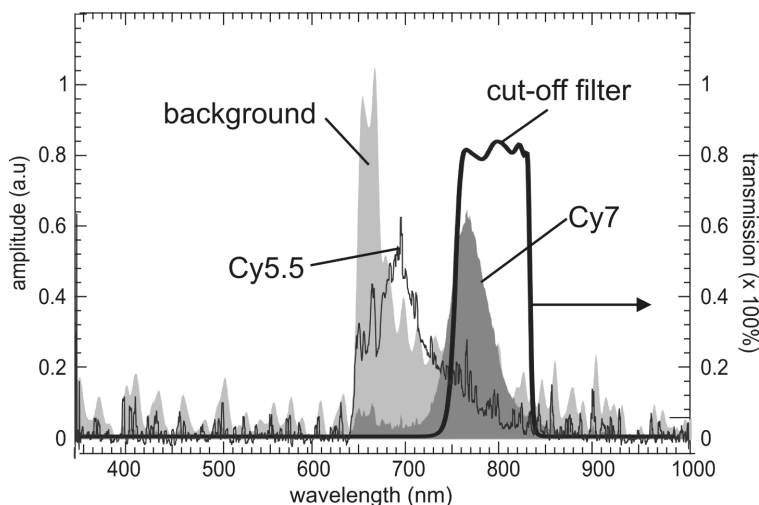


Figure 3: Spectra of light leaving the fiber towards the detector. As indicated: Spectrum of the background caused by inelastic scattering of the excitation light in the optical fiber as well as the fluorescence emission of solutions of Cy5.5 and Cy7 as well as the transmission spectrum of the bandpass filter (see Figure 2, 3, XF3307, Omega Optical). The sharp cutoff towards shorter wavelength in the background as well as the Cy5.5 fluorescence spectrum at ≈ 640 nm is due to a notch filter centered at 632 nm.

Supporting Information 4

Position optimization

Since the velocity profile in the analyte solution varies as a function of the distance to the rotor, we expect the detection rate of the setup to be strongly dependent both on the stirring rate of the rotor and on the fiber position relative to the rotor. Therefore, to optimize the detection rate, an optimal fiber position and stirring rate has been determined. To this end, series of 30 s time traces have been recorded at different axial and radial positions of the fiber at a fixed stirring rate of 20000 rpm. After each measurement the fiber was moved by $50 \mu\text{m}$ to a new position. Figure 4 shows the result

of the radial (x) variation of the fiber position. Coordinates have been determined by measuring the distance to the upper corner of the rotor, counting outwards (see inset in Figure 4). A maximum in the number of counted bursts is found at a fiber position of 0.45 mm when moving from 0.6 mm to 0.05 mm and at a fiber position of 0.35 mm when moving back, respectively. Accordingly, a position of $x=0.4$ mm has been chosen for all subsequent measurements. The optimal position in axial (y) direction has been determined in similar experiments. A set of measurements has been performed changing the height of the fiber in steps of $200\ \mu\text{m}$. A maximum is found at a position of 0.3 mm as seen in figure Figure 4. Accordingly, for subsequent measurements a position of $y=0.3$ mm has been chosen. In comparison to the radial fiber scan, the y -scan is much broader. Therefore the vertical position of the fiber can be considered not to be as critical for optimal detection. In similar experiments, time traces have been recorded for different stirring rates but at fixed radial and vertical position. At stirring rates above ≈ 16000 rpm the number of detected molecules begins to saturate (see Figure 5). A rate of 20000 rpm, well within saturation, has therefore been chosen for the experiments. We have also performed an autocorrelation analysis of time traces recorded at different stirring speed (1 pM concentration) which shows increasing burst width for increasing stirring speed indicating the formation of vortices. The results are displayed in Fig. Figure 5 (b)

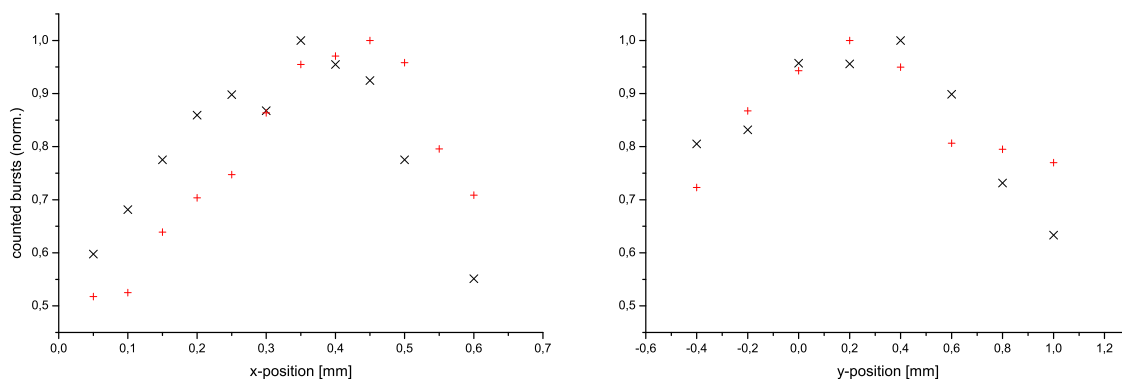


Figure 4: Dependence of the number of fluorescence bursts on the radial fiber position (left) and vertical fiber position (right). The position is determined outwards from the edge of the rotor. (+) has been measured form high to low values, (x) from low to high values.

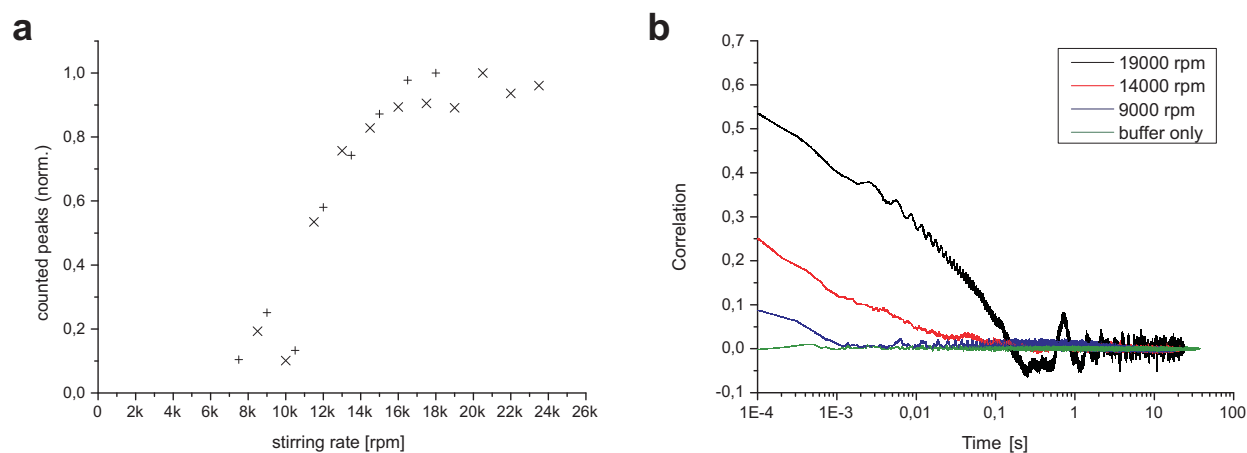


Figure 5: **a:**Dependence of detected molecules on the stirring rate at fixed position. (+) has been measured from high to low values, (x) from low to high values.**b:** Autocorrelation of time traces recorded at 1 pM concentration showing increasing fluorescence burst width for increasing stirring rates indicating the formation of vortices.

Supporting Information 5

Data analysis

The recorded time traces are evaluated using a burst-detection and counting algorithm described in Grange et al.⁵. In brief, the algorithm distinguishes between the distribution of the burst histogram and the distribution of the background by directly using the time-trace including all single-molecule bursts to obtain a first guess to describe the background alone. Every burst above a certain, predefined threshold χ is then counted and subsequently removed from the time trace using a routine implemented in Labview (National Instruments). In the next iteration, the time-trace - now without the previously detected bursts - is again used to determine an already much better estimate for the background distribution. These steps are repeated until all bursts have been counted and the background distribution is not improved any more by removing more bursts. An important factor is the threshold χ that defines the allowed overlap between the background and the burst distributions. For low χ , few (down to <1) wrong positive bursts will be detected, inevitably leading to some amount of signal bursts in the overlap region of the two distributions to be missed. A higher χ results in the detection of more bursts, but also some wrong positive (background) bursts will be

detected, which depending on the application, may however be tolerable. Prior to evaluating the experimental data, therefore a value for the threshold χ has to be chosen. By analyzing a typical data set for different values of χ , a value of 400 was found to be a reasonable choice for all but the smallest concentrations investigated in the present study. At this value, the root mean squared error (RMSE), providing an estimate of the quality of the fit to the resulting Poissonian background distribution with all bursts removed, is significantly reduced while the number of detected bursts considerably increased. At the same time the number of wrong positives stays comparatively low. For further details see⁵.

References

- (1) Lukosz, W.; Kunz, R. *J. Opt. Soc. Am.* **1977**, *67*, 1615–1619.
- (2) Novotny, L.; Hecht, B. *Principles of Nano-Optics*; Cambridge University Press, 2006.
- (3) Seidel, C. A. M.; Schulz, A.; Sauer, M. H. M. *The Journal of Physical Chemistry* **1996**, *100*, 5541–5553.
- (4) Tyagi, S.; Marras, S.; Kramer, F. *Nucleic Acids Research* **2002**, *30*, e122.
- (5) Grange, W.; Haas, P.; Wild, A.; Calame, M.; Hegner, M.; Hecht, B. *J. Phys. Chem. B* **2008**, *112*, 7140–7144.